

## Electroexcitation of rotational bands in $^{18}\text{O}$

D. M. Manley

*Department of Physics and Center for Nuclear Research, Kent State University, Kent, Ohio 44242*

D. J. Millener

*Brookhaven National Laboratory, Upton, New York 11973*

B. L. Berman

*Department of Physics, The George Washington University, Washington, D.C. 20052*

W. Bertozzi, T. N. Buti,<sup>(a)</sup> J. M. Finn,<sup>(b)</sup> F. W. Hersman,<sup>(c)</sup> C. E. Hyde-Wright,<sup>(d)</sup> M. V. Hynes,<sup>(e)</sup>  
J. J. Kelly,<sup>(f)</sup> M. A. Kovash,<sup>(g)</sup> S. Kowalski, R. W. Lourie,<sup>(h)</sup> B. Murdock,<sup>(i)</sup> B. E. Norum,<sup>(h)</sup>  
B. Pugh,<sup>(j)</sup> and C. P. Sargent<sup>(k)</sup>

*Department of Physics and Laboratory for Nuclear Science, Massachusetts Institute of Technology,  
Cambridge, Massachusetts 02139*

(Received 18 September 1989)

The fourth  $2^+$  state in  $^{18}\text{O}$  at an excitation energy of 8.21 MeV has been studied by high-resolution electron scattering. The Coulomb form factor for this state was measured in the momentum-transfer range  $0.9 \leq q \leq 2.1 \text{ fm}^{-1}$  and the extracted  $B(C2)\uparrow$  value was determined to be  $7.3 \pm 4.2 e^2 \text{fm}^4$ . The level at 8.21 MeV is identified as a four-particle, two-hole (4p2h) state of the type  $p^{-2}(sd)^4$ . Form-factor measurements in the range  $1.0 \leq q \leq 1.9 \text{ fm}^{-1}$  are also presented for a strongly excited normal-parity state at 9.36 MeV. Preliminary measurements of the differential cross section for exciting this state by 135-MeV protons suggest a  $2^+$  assignment; the measured Coulomb form factor of this state allows it to be identified as the best experimental candidate for a predicted  $K=2$  4p2h state with the four  $sd$ -shell nucleons coupled to  $T=0$ . The excitation of these states and other members of rotational bands in  $^{18}\text{O}$  are discussed within the framework of structure models. Shell-model calculations for the  $C4$  form factors of the first three  $4^+$  states in  $^{18}\text{O}$  are compared to existing data.

### I. INTRODUCTION

The three  $2^+$  states in  $^{18}\text{O}$  with excitation energies of 1.98, 3.92, and 5.26 MeV have received much attention in the last decade.<sup>1</sup> Of particular interest has been the excitation of these levels by the inelastic scattering of medium-energy electrons,<sup>2</sup> protons,<sup>3</sup> and pions<sup>4</sup> and the use of combined electromagnetic and hadronic data to obtain empirical<sup>2,4,5</sup> or test model<sup>2,4,6</sup> proton and neutron transition densities. While the microscopic structures of these states are now believed to be well understood, with the essential features of the analysis by Lawson, Serduke, and Fortune<sup>7</sup> remaining intact, the structure of the fourth  $2^+$  state, which lies 8.21 MeV above the ground state, is less certain. We have studied the 8.21-MeV state by performing an electron scattering experiment at the MIT-Bates Linear Accelerator Center. The main details of the experiment and data analysis are presented elsewhere.<sup>8</sup> Here we present and discuss the first measurements of the longitudinal or Coulomb form factors for the  $2_4^+$  state and a state at 9.36 MeV, which we suggest is also a  $2^+$  state. An extended shell-model calculation using a complete  $(sd)^2$  plus truncated  $2\hbar\omega$  basis was performed to investigate the band structures of positive-parity states; predicted  $C4$  form factors are compared with existing data for the first three  $4^+$  states.

In the simple shell model, the low-lying positive-parity

states of  $^{18}\text{O}$  are formed by adding two valence neutrons to a closed-shell core of  $^{16}\text{O}$ . Table I gives the positive-parity spectrum predicted with the Chung-Wildenthal (CW) interaction<sup>9</sup> in this "0 $\hbar\omega$ " basis. The predicted  $2^+$  states at 2.00 and 4.03 MeV correspond to the levels observed experimentally at 1.98 and 3.92 MeV, respectively. The next level observed experimentally occurs at 5.26 MeV and has a mainly 4p2h structure. From Table I, it can be seen that the 0 $\hbar\omega$  calculation predicts that the next 2p0h  $2^+$  state should occur at about 9.45 MeV and have the dominant structure,  $d_{5/2}d_{3/2}$ . Consider now the corresponding predictions for the  $4^+$  states. The lowest predicted  $4^+$  state at 3.52 MeV corresponds to the level observed experimentally at 3.55 MeV. The next level observed experimentally is the mainly 4p2h state at 7.12 MeV. One other  $4^+$  state whose dominant structure is  $d_{5/2}d_{3/2}$  is predicted to occur at 8.21 MeV. This level corresponds to a state that was observed experimentally at 9.0 MeV in the  $^{16}\text{O}(t,p)^{18}\text{O}$  and  $^{17}\text{O}(d,p)^{18}\text{O}$  reactions.<sup>10</sup> The 3.55- and 9.0-MeV  $d^2$  levels are selectively excited in heavy-ion two-neutron transfer reactions, such as the  $^{16}\text{O}(^{18}\text{O},^{16}\text{O})^{18}\text{O}$  reaction.<sup>11</sup> The 9.0-MeV state was *not* observed in the electron scattering experiment, a point that we return to later.

The leading or lowest representation in the  $\text{SU}_3$  basis for four particles in the  $sd$  shell and two holes in the  $p$  shell is  $(\lambda\mu)=(82)$ . This representation contains a  $K=0$

TABLE I. Theoretical  $0\hbar\omega$  intensities (%) for positive-parity states in  $^{18}\text{O}$  calculated with the Chung-Wildenthal interaction in an  $(sd)^2$  basis. The predicted excitation energies are given in MeV.

$E_x$	$J_n^\pi$	$(d_{5/2})^2$	$d_{5/2}s_{1/2}$	$(s_{1/2})^2$	$d_{5/2}d_{3/2}$	$s_{1/2}d_{3/2}$	$(d_{3/2})^2$
0.00	$0_1^+$	74.9		17.1			8.0
4.01	$0_2^+$	16.4		82.8			0.8
14.38	$0_3^+$	8.6		0.1			91.2
9.45	$1_1^+$				97.0	3.0	
10.10	$1_2^+$				3.0	97.0	
2.00	$2_1^+$	67.4	25.6		0.4	4.9	1.7
4.03	$2_2^+$	29.6	67.6		0.5	2.3	0.0
9.45	$2_3^+$	1.7	0.4		87.6	8.6	1.7
10.25	$2_4^+$	0.4	5.5		8.9	84.2	1.0
14.49	$2_5^+$	0.9	0.8		2.7	0.1	95.5
5.53	$3_1^+$		99.3		0.7		
9.51	$3_2^+$		0.7		99.3		
3.52	$4_1^+$	91.2			8.8		
8.21	$4_2^+$	8.8			91.2		

band and a  $K=2$  band, with the  $K=0$  band expected to occur lower in energy. It is now well established that the low-lying positive-parity levels in  $^{18}\text{O}$  at 3.63 MeV ( $0_2^+$ ), 5.26 MeV ( $2_3^+$ ), and 7.12 MeV ( $4_2^+$ ) are predominantly 4p2h states.<sup>7</sup> These so-called "intruder states" can be identified as members of the predicted  $K=0$  band; the dominant structures of these states also can be described by the weak-coupling configurations,  $^{20}\text{Ne}(J^\pi) \otimes ^{14}\text{C}(0^+)$ , where  $J^\pi=0^+$ ,  $2^+$ , or  $4^+$ , which leads to large  $\alpha$ -particle spectroscopic factors for  $^{14}\text{C}+\alpha$ . These states also have appreciable components of  $^{20}\text{Ne}(2^+) \otimes ^{14}\text{C}(2^+)$  and other parentages. Analogous states in  $^{16}\text{O}$  are found at 6.05 MeV ( $0_2^+$ ), 6.92 MeV ( $2_1^+$ ), and 10.36 MeV ( $4_1^+$ ); these predominantly 4p4h states are the lowest members of the  $K=0$  band contained in the leading  $\text{SU}_3$  representation (84) for four particles in the  $sd$  shell and four holes in the  $p$  shell. The (84) representation also contains a  $K=2$

band and a  $K=4$  band. The  $2_2^+$  state in  $^{16}\text{O}$  at 9.84 MeV can be identified as the head of this  $K=2$  band. We argue in Sec. II that a normal-parity state in  $^{18}\text{O}$  at 9.36 MeV is the best experimental candidate for the corresponding head of the  $K=2$  band contained in the (82) representation. A feature of these  $K=2$  bands in  $^{16}\text{O}$  and  $^{18}\text{O}$  is that they contain very small  $^{20}\text{Ne}(J^\pi) \otimes ^{12,14}\text{C}(0^+)$  components, and the  $2^+$  states have large  $0^+ \otimes 2^+$  and  $2^+ \otimes 2^+$  components. A consequence is that  $0^+ \rightarrow K=2, 2^+$  transitions are dominated by  $1p \rightarrow 1p$  transitions, as is evident in the form factor for the 9.84-MeV  $2_2^+$  state in  $^{16}\text{O}$ , which is strikingly different in shape from those of the  $2^+$  levels at 6.92 and 11.52 MeV.<sup>12</sup>

Excitation energies of particle-hole states in  $^{18}\text{O}$  can be estimated by using the Bansal-French-Zamick formula for weak-coupling configurations,<sup>13,14</sup>

$$E_x \{ [(sd)^m J_p T_p \otimes p^{-n} J_h T_h ] JT \} = E_B(16+m) + E_B(16-n) - E_B(^{16}\text{O}) - E_B(^{18}\text{O}) + Amn + B \langle T_p \cdot T_h \rangle. \quad (1)$$

Here  $E_x$  is the excitation energy of a state with the weak-coupling structure of  $m$   $sd$ -shell particles with spin  $J_p$  and isospin  $T_p$  coupled to  $n$   $p$ -shell holes with spin  $J_h$  and isospin  $T_h$ . The energy of the particle-hole state, so formed, with spin  $J$  and isospin  $T$  is a combination of binding energies (including excitation energies) and the expectation value of the particle-hole interaction; the coefficients,  $A$  and  $B$  in Eq. (1) were found<sup>14</sup> to have values of 0.23 and 5.02 MeV, respectively, by requiring approximate agreement between the calculated and experimental energies of the first  $T=0$  and  $T=2$  excited states in  $^{16}\text{O}$ . Table II compares calculated and experimental excitation energies for several weak-coupling configurations in  $^{18}\text{O}$ . The experimental values are from Ref. 1 and the calculated values use binding energies ( $E_B$ ) from the tables of Wapstra and Bos.<sup>15</sup> The first four states in Table II are members of the  $K=0$  band already discussed; for these states, the four  $sd$ -shell nucleons cou-

ple to  $T=0$ . The next three states arise from coupling two  $p$ -shell holes to four  $sd$ -shell nucleons with  $T=1$ . As we discuss later this configuration probably forms a large component of the  $2_4^+$  state at 8.21 MeV. For the two  $1^+$  states in Table II, the  $sd$ -shell nucleons have the configurations of the  $1_1^+$  state in  $^{20}\text{F}$  at 1.06 MeV and its analog in  $^{20}\text{Ne}$  at 11.26 MeV, which is the most prominent  $1^+$  state in the  $^{20}\text{Ne}(e, e')^{20}\text{Ne}$  reaction.<sup>16</sup> The narrow state seen at 8.82 MeV in the  $^{18}\text{O}(p, p')^{18}\text{O}$  reaction<sup>17</sup> is a strong candidate for the lowest 4p2h  $1^+; 1$  state in  $^{18}\text{O}$  since the  $d_{5/2}d_{3/2}$  configuration should have a considerable neutron width and is expected at higher excitation energy (see, e.g., Table I). The 4p2h  $1^+; 2$  state in  $^{18}\text{O}$  is found<sup>18</sup> at 18.87 MeV with  $B(M1) \uparrow = 0.28(4) \mu_N^2$ , a value that is consistent with the 10–20% 4p2h admixture in the  $^{18}\text{O}$  ground state deduced from analyses of other data (see later). With the  $1^+$  states so identified, a  $2^+$  state is expected below 8.8 MeV for which a candidate

TABLE II. Comparison of calculated and experimental excitation energies (MeV) for selected 4p2h states in  $^{18}\text{O}$ . The experimental values are from Ref. 1 and the notation for weak-coupling configurations is that of Ref. 14. (An asterisk denotes isobaric analog states with  $T=1$ .)

$J^\pi$	$T$	Configuration	$E_x$ (Calc.)	$E_x$ (Expt.)
		$(sd)_{T=0}^4 \otimes p_{T=1}^{-2}$		
$0^+$	1	$^{20}\text{Ne}(0^+) \otimes ^{14}\text{C}(0^+)$	3.34	3.63
$2^+$	1	$^{20}\text{Ne}(2^+) \otimes ^{14}\text{C}(0^+)$	4.97	5.26
$4^+$	1	$^{20}\text{Ne}(4^+) \otimes ^{14}\text{C}(0^+)$	7.59	7.12
$6^+$	1	$^{20}\text{Ne}(6^+) \otimes ^{14}\text{C}(0^+)$	12.12	11.69
		$(sd)_{T=1}^4 \otimes p_{T=1}^{-2}$		
$2^+$	1	$[^{20}\text{Ne}^*(2^+) \otimes ^{14}\text{C}(0^+) - ^{20}\text{F}(2^+) \otimes ^{14}\text{N}^*(0^+)]/\sqrt{2}$	8.05	8.21
$1^+$	1	$[^{20}\text{Ne}^*(1^+) \otimes ^{14}\text{C}(0^+) - ^{20}\text{F}(1^+) \otimes ^{14}\text{N}^*(0^+)]/\sqrt{2}$	9.07	8.82
$1^+$	2	$[^{20}\text{Ne}^*(1^+) \otimes ^{14}\text{C}(0^+) + ^{20}\text{F}(1^+) \otimes ^{14}\text{N}^*(0^+)]/\sqrt{2}$	19.11	18.87

exists at 8.21 MeV. We now argue that the levels in  $^{18}\text{O}$  at 8.21 and 9.36 MeV possess a number of properties that enable us to identify them as the 4p2h  $2^+$  states already described.

## II. ANALYSIS AND DISCUSSION

In the standard plane-wave Born approximation, total form-factor measurements for normal-parity states in even-even nuclei can be separated into longitudinal and transverse components:

$$|F|^2 = \frac{Q^4}{q^4} |F_{CJ}(q)|^2 + \left[ \frac{Q^2}{2q^2} + \tan^2 \frac{\theta}{2} \right] |F_{EJ}(q)|^2, \quad (2)$$

where  $Q^2$  and  $q^2$  are the square of the four- and three-momentum transfer, respectively, and  $\theta$  is the electron scattering angle. We fitted the total form-factor measurements with a polynomial-times-Gaussian parametrization, as discussed, for example, in Refs. 8, 12, and 14:

$$F_{CJ}(q) = \frac{\sqrt{4\pi}}{Z} \frac{q^J}{(2J+1)!!} f_{\text{c.m.}}(q) f_N(q) e^{-y} \sum_{n=0}^N A_n y^n, \quad (3)$$

$$F_{EJ}(q) = \frac{\sqrt{4\pi}}{Z} \frac{q^J}{(2J+1)!!} \left[ \frac{J+1}{J} \right]^{1/2} \times \frac{\omega}{q} f_{\text{c.m.}}(q) f_N(q) e^{-y} \sum_{n=0}^{N+1} B_n y^n, \quad (4)$$

where  $y = (qb/2)^2$ . This parametrization was chosen to facilitate comparisons with shell-model calculations that use harmonic-oscillator wave functions. The oscillator parameter was determined<sup>8</sup> to have the value,  $b = 1.879 \pm 0.023$  fm, by simultaneously fitting form-factor measurements for 15 normal-parity states in  $^{18}\text{O}$ . The measurements were obtained by exposing BeO targets, enriched up to 90.8% in  $^{18}\text{O}$ , to intense electron beams at the M.I.T.-Bates Linear Accelerator Center. For the 8.21- and 9.36-MeV states discussed here, mea-

surements were performed at scattering angles of  $90^\circ$  and  $160^\circ$  with beam energies between 120 and 300 MeV. All measurements presented here for the 9.36-MeV state were obtained with a  $^9\text{Be}^{18}\text{O}$  target that had an average thickness of 47.3 mg/cm<sup>2</sup>. The width of the 9.36-MeV state was found to be  $\leq 20$  keV and the uncertainty in its excitation energy was  $\pm 0.02$  MeV.

### A. The level at 8.21 MeV

Table III summarizes the expansion coefficients,  $A_n$  and  $B_n$ , for the longitudinal and transverse form factors of the  $2_4^+$  level at 8.21 MeV. The first column of Table III gives the results of a fit in which all expansion coefficients up to  $n=2$  are allowed to vary. This fit gives a good representation of the extracted Coulomb form factor, which is shown in Fig. 1. However, the  $\chi^2$  per degree of freedom is large ( $\chi^2/\nu = 6.1$ ), and it is clear that all five expansion coefficients cannot be extracted from the data. In fact, the fitted  $B_n$  coefficients give rise to an unphysical  $|F_T|^2 = |F_{E2}|^2$ , which exhibits three maxima at  $q_{\text{eff}} \approx 0.3, 1.0, \text{ and } 2.0$  fm<sup>-1</sup>. In addition,  $|F_T|^2$  points obtained by subtracting the fitted  $|F_L|^2 = |F_{C2}|^2$  values show considerable scatter and do not yield a clearly defined transverse form factor. The second column of Table III gives the result of a fit in which  $B_1$  and  $B_2$  are set to zero. In this case,  $A_2$  is still undefined. The third and fourth columns of Table III give the results of fits with  $A_2$  also set to zero for two values of the oscillator parameter,  $b = 1.879$  fm from the omnibus fit to 15 states and  $b = 1.821$  fm deduced<sup>19</sup> from the measured rms charge radius of 2.794 fm (Ref. 20).

The coefficient  $A_0 = B_0$  corresponds to  $B(C2)\uparrow = 7.3 \pm 4.2 e^2 \text{fm}^4$ , where the quoted uncertainty takes into account the model dependency of our parametrization and, in particular, the fact that there are no data points for  $q_{\text{eff}} < 0.85$  fm<sup>-1</sup>. The value obtained for  $B(C2)\uparrow$  is in agreement with the result,  $B(E2)\downarrow = 0.9 \pm 0.3$  W.u. or  $B(C2)\uparrow = 13 \pm 4 e^2 \text{fm}^4$ , obtained from the  $^{14}\text{C}(\alpha, \gamma)^{18}\text{O}$  measurement of Gai *et al.*<sup>21</sup>

TABLE III. Expansion coefficients (in  $\text{efm}^2$ ) for the longitudinal and transverse electric form factors of the  $2_4^+$  state in  $^{18}\text{O}$  at 8.21 MeV, fitted to 23 data points at  $\theta=90^\circ$  and six data points at  $\theta=159.8^\circ$ . The value of the oscillator parameter  $b$  obtained by fitting 15 levels simultaneously was  $1.879(23)$  fm (Ref. 8), while that obtained from the rms charge radius is  $1.821$  fm (Ref. 19).

Quantity	Value <sup>b</sup>			
$b$	1.879	1.879	1.879	1.821
$A_0$	2.71(26)	2.79(20)	2.89(8)	2.78(8)
$A_1$	-0.33(30)	-0.46(22)	-0.59(4)	-0.66(4)
$A_2$	-0.08(8)	-0.03(6)	0	0
$B_1$	-8.6(43)	0	0	0
$B_2$	3.9(17)	0	0	0
$\chi^2/\nu$	6.13	5.89	5.74	5.70
$B(C2)\uparrow^c$	7.3(14)	7.8(12)	8.4(5)	7.7(4)

<sup>a</sup>Uncertainties in the last significant figure are given in parentheses.

<sup>b</sup>Parameters set to zero are so indicated.

<sup>c</sup> $B(C2)\uparrow = A_0^2 = B_0^2$  in  $e^2\text{fm}^4$ . Only the uncertainties due to fitting are represented.

Figure 1 shows the extracted Coulomb form factor for the  $2_4^+$  state in  $^{18}\text{O}$  at 8.21 MeV (the solid curve was generated from coefficients listed in the first column of Table III). This state's measured transverse form factor is negligible (within experimental uncertainties), as are those of the lowest three  $2^+$  states.<sup>2</sup> The only structures at all likely for  $2^+$  states in  $^{18}\text{O}$  excited by Coulomb excitations are a mainly  $d_{5/2}d_{3/2}$  configuration or mainly  $4p2h$  configurations of the two types discussed in Sec. I. If the structure of the 8.21-MeV level is as we suggest in Table II, then its  $C2$  form factor should be similar to those of other  $2^+$  states excited by  $C2$  transitions within the  $sd$  shell. The shape given by the harmonic-oscillator  $1d \rightarrow 1d$  form factor, with a polynomial  $1 - \frac{2}{3}y$ , is approximately correct, as is that of an empirical  $1d \rightarrow 1d$  form factor extracted by Norum *et al.*,<sup>2</sup> with a minimum around  $q_{\text{eff}} = 2.1 \text{ fm}^{-1}$ ; thus, the shape expected for the

excitation of the  $d_{5/2}d_{3/2}$  configuration is also consistent with the data. However, in the Chung-Wildenthal ( $sd$ )<sup>2</sup> model,  $B(C2)\uparrow$  is only  $2.1 e^2\text{fm}^4$  (for  $\delta e_n = 0.5$  and  $b = 1.821 \text{ fm}$ ) and, more tellingly, a  $d_{5/2}d_{3/2}$  state at 8.21 MeV should be strongly populated in the  $^{17}\text{O}(d,p)^{18}\text{O}$  reaction, contrary to the experimental results.<sup>10</sup> The very small neutron width (quoted as  $6.2 \times 10^{-4}\%$  of the Wigner limit<sup>22</sup>) of the 8.21-MeV level also argues against a significant  $d_{5/2}d_{3/2}$  component. These observations clearly reveal that the 8.21-MeV state *must* be a multiparticle-multiparticle configuration, since it is inconsistent with a mainly two-particle configuration. Finally, we note that the experimental excitation energy agrees very well with the weak-coupling-model prediction of 8.05 MeV (Table II).

We conclude from the preceding discussion that an identification of the  $4p2h$   $2^+$  state with the 8.21-MeV state in  $^{18}\text{O}$  is consistent with the measured ( $e, e'$ ) form factor, while a  $d_{5/2}d_{3/2}$  assignment is inconsistent with the properties of the 8.21-MeV level on several counts. The very small  $\alpha$  width (quoted as 0.9% of the Wigner limit<sup>22</sup>) of the 8.21-MeV level is also consistent with the expectation of a very small  $^{14}\text{C} + \alpha$  spectroscopic factor.

### B. The level at 9.36 MeV

At excitation energies between 9 and 14 MeV, the most prominent states in the spectrum (Fig. 2) for 194.3-MeV electrons scattered from  $^{18}\text{O}$  at  $90^\circ$  ( $q \approx 1.3 \text{ fm}^{-1}$ ) are a level at 9.36 MeV and one at 11.65 MeV. The measured widths of these levels in this work are  $\leq 20 \text{ keV}$  and  $76 \pm 8 \text{ keV}$ , respectively. The observed strengths of these states indicate that they have  $J \leq 4$ ; both states have normal parity as indicated by their mainly Coulomb form factors. The shape of the Coulomb form factor for the 9.36-MeV level was determined well by these measurements. Table IV summarizes the expansion coefficients,  $A_n$  and  $B_n$ , for the longitudinal and transverse form factors of the level at 9.36 MeV and Fig. 3 shows the extracted Coulomb form factor; also shown in Fig. 3 are curves obtained by fitting the data under assumptions that the level is either a  $2^+$ ,  $3^-$ , or  $4^+$  state. Its shape is

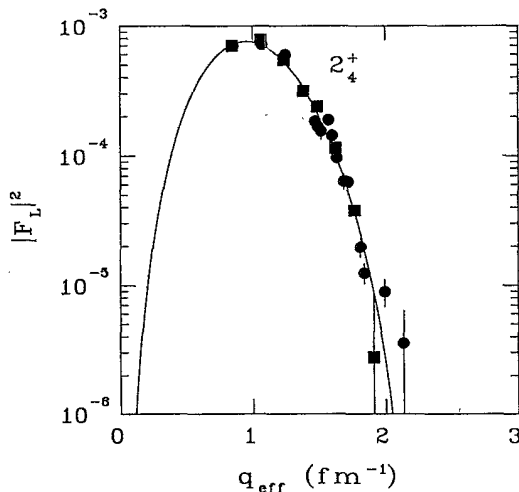


FIG. 1. The solid curve shows the fitted Coulomb form factor for the  $2_4^+$  state at 8.21 MeV. Solid squares indicate measurements of Coulomb form factors from this analysis and solid circles indicate measurements from an earlier analysis.<sup>2</sup>

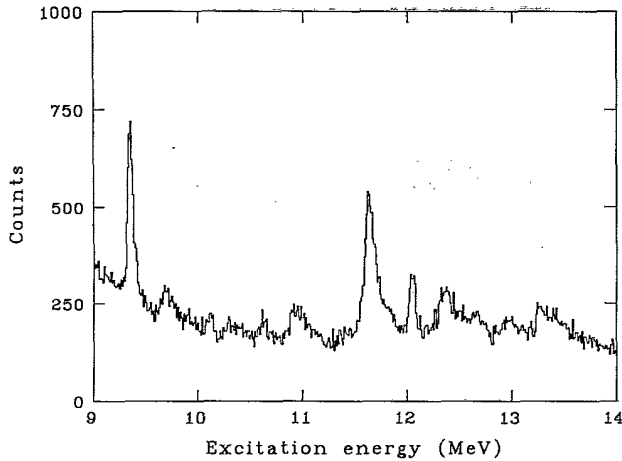


FIG. 2. A spectrum for 194.3-MeV electrons scattered from  ${}^9\text{Be}^{18}\text{O}$  at  $\theta=90^\circ$ , corresponding to  $q_{\text{eff}}=1.4 \text{ fm}^{-1}$ . Note the strongly excited levels at 9.36 and 11.65 MeV.

consistent with any of these assignments; however, the large  $C4$  strength implied assuming  $J^\pi=4^+$  argues against that assignment.

Preliminary measurements<sup>23</sup> of the differential cross section for exciting the levels in  ${}^{18}\text{O}$  at 8.21 and 9.36 MeV by 135-MeV protons are shown in Fig. 4. The similarity of the angular distributions with each other and with angular distributions for known  $2^+$  states in  ${}^{16}\text{O}$  (Ref. 24) suggest *strongly* that the level at 9.36 MeV is also a  $2^+$  state. With this assignment, our electron-scattering measurements indicate a  $B(C2)\uparrow$  of  $2.2\pm 1.3 e^2\text{fm}^4$ , where the quoted uncertainty takes into account the model dependency of our parametrization and, in particular, the fact that there are no data points for  $q_{\text{eff}} < 1.03 \text{ fm}^{-1}$ . The form factor for the 9.36-MeV level (Fig. 3) is similar in shape to that of the  $2_2^+$  level at 9.84 MeV in  ${}^{16}\text{O}$  (Ref. 12) and suggests that this state is excited mainly by a  $1p \rightarrow 1p$  transition. In contrast,<sup>2</sup> the  $C2$  form factors of the three  $2^+$  states in  ${}^{18}\text{O}$  at 1.98, 3.92, and 5.26 MeV all exhibit minima below  $q_{\text{eff}}=2 \text{ fm}^{-1}$ .

In order to investigate the band structures of positive-

TABLE IV. Expansion coefficients (in  $e\text{fm}^J$ ) for the longitudinal and transverse electric form factors of the state in  ${}^{18}\text{O}$  at 9.36 MeV, fitted to six data points at  $\theta=90^\circ$  and four data points at  $\theta=159.8^\circ$ . The assumed spin and parity of the state are so indicated; the value of the oscillator parameter  $b$  was 1.879 fm.

Quantity	Value		
$J^\pi$	$2^+$	$3^-$	$4^+$
$A_0$	1.47(15)	12.78(94)	112(9)
$A_1$	0.36(8)	-1.14(42)	-23(4)
$B_1$	1.98(81)	7.3(53)	28(55)
$\chi^2/\nu$	1.09	1.32	2.69
$B(CJ)\uparrow^a$	2.16(45)	162(24)	$1.25(21)\times 10^4$

<sup>a</sup> $B(CJ)\uparrow = A_0^2 = B_0^2$  in  $e^2\text{fm}^{2J}$ . Only the uncertainties due to fitting are represented.

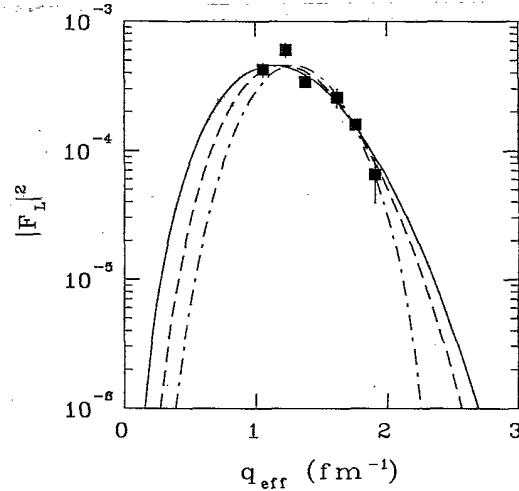


FIG. 3. Coulomb form-factor measurements for the state in  ${}^{18}\text{O}$  at 9.36 MeV. The solid, dashed, and dot-dashed curves were obtained by fitting the data under the assumptions that the level is a  $2^+$ ,  $3^-$ , or  $4^+$  state, respectively.

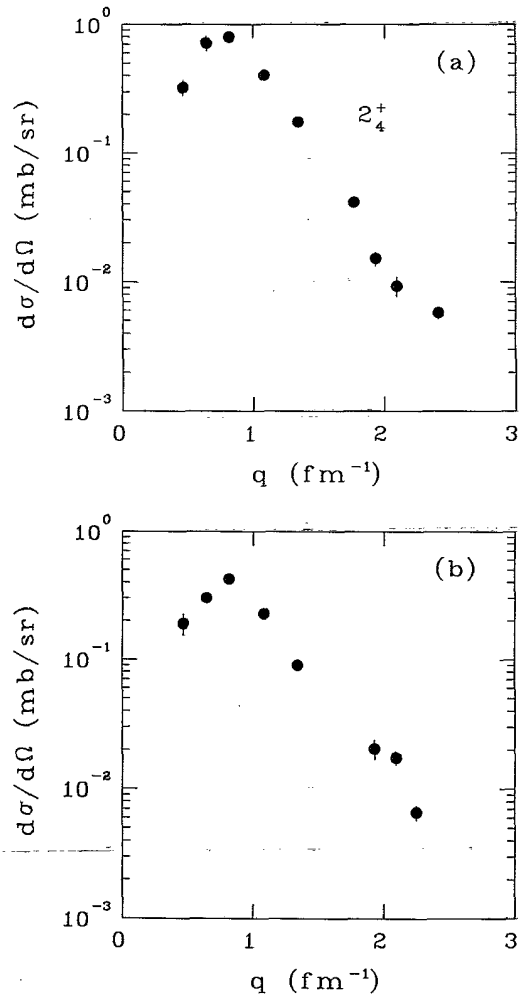


FIG. 4. Measurements of the differential cross section for scattering 135-MeV protons from the levels in  ${}^{18}\text{O}$  at (a) 8.21 MeV and (b) 9.36 MeV.

TABLE V. Collective band structures in  $^{18}\text{O}$ . Theoretical  $2\hbar\omega$  intensities (%) in the  $\text{SU}_3$  basis and excitation energies (MeV) were calculated in a full  $0\hbar\omega$  plus truncated  $2\hbar\omega$  basis as discussed in the text.

$J^\pi$	$E_x$ (Theory)	$E_x$ (Expt.)	$2\hbar\omega$ (%)	(82)	(90)	(71)	(63)	(44)
<b><math>K=0</math> band</b>								
$0^+$	3.49	3.63	87.9	62.2	15.6	6.9	2.6	0.8
$2^+$	4.90	5.26	91.3	63.0	15.4	7.0	3.4	1.5
$4^+$	7.44	7.12	80.2	54.9	11.8	6.3	4.5	2.8
$6^+$	11.57	11.69	100.0	64.2	13.5	12.4	9.2	0.8
<b><math>K=2</math> band</b>								
$2^+$	9.49	9.36	95.8	79.8	1.3	6.7	5.0	3.0
$3^+$	10.47		99.9	79.9	2.5	8.1	6.3	3.0
$4^+$	11.50		99.5	72.0	4.6	11.8	6.4	4.6
$5^+$	13.20		100.0	58.1	2.4	9.4	24.4	5.7
$6^+$	14.49		100.0	51.4	6.5	28.9	11.4	1.8

parity states in  $^{18}\text{O}$  more fully, we also performed a more extensive shell-model calculation using a complete  $(sd)^2$  plus truncated  $2\hbar\omega$  basis  $[(\lambda\mu)=(82), (90), (71), (63), \text{ and } (44)]$  with total spin  $S \leq 1$ . In this basis, the wave functions for positive-parity states have the general form,

$$|\pi=+\rangle = \alpha|(sd)^2\rangle + \beta|p^{-2}(sd)^4\rangle + \gamma|p^{-1}(sd)^2(pf)\rangle. \quad (5)$$

The predicted compositions and excitation energies of the low-lying  $K=0$  and  $K=2$  bands having large components of the (82) representation are listed in Table V. The  $K=0$  states are all predicted to have large  $^{14}\text{C}(\text{g.s.}) + \alpha$  spectroscopic factors ( $0.15 < \mathcal{S}_\alpha < 0.18$ ) and the levels listed as their experimental counterparts are all strongly populated in  $\alpha$ -transfer reactions on a  $^{14}\text{C}$  target.<sup>25-27</sup> A breakdown of the contributions to the polynomial coefficients  $A_0$  and  $A_1$  for transitions from the lowest  $2\hbar\omega$   $0^+$  state to the  $2\hbar\omega$   $2^+$  states is given in Table VI. It is clear that  $1p \rightarrow 1p$  transitions dominate in the

excitation of the  $K=2$   $2^+$  state. Estimates of the intensity of the  $4p2h$   $0^+$  component in the ground state range from just over 10% (Ref. 7) to just under 19% (Ref. 6). An admixture of 15%, with the  $A_0$  coefficient from Table VI, gives  $B(C2)\uparrow = 7.9 e^2\text{fm}^4$  for the excitation of the pure  $2\hbar\omega$  state identified with the 9.36-MeV  $2^+$  state of  $^{18}\text{O}$ . A further range of variation in the theoretical prediction arises because the  $B(C2)\uparrow$  also scales as  $(1 + \delta e_p)^2 b^4$ , where  $1 + \delta e_p$  is the effective charge appropriate for a  $p$ -shell proton transition; e.g., the value  $1 + \delta e_p \approx 1.15$  found for  $^{13}\text{C}$  (Ref. 28) is lower than the value 1.5 used in Table VI and would imply  $B(C2)\uparrow = 4.7 e^2\text{fm}^4$ .

The shell-model prediction of 9.49 MeV (Table V) for the excitation energy of the  $K=2$  band head agrees very well with the experimental value of 9.36 MeV. As already noted, the shell-model wave function for this state is dominated by the (82) representation in an  $\text{SU}_3$  basis. In this calculation, the  $K=2$   $2^+$  state mixes weakly with the predicted nearby  $(sd)^2$  configurations at 9.2 MeV

TABLE VI. One-body density-matrix elements and polynomial coefficients for  $0^+ \rightarrow 2^+$  transitions between  $4p2h$  states in  $^{18}\text{O}$ . Results for the  $K=0$   $2^+$  state are given first, followed by results for the  $K=2$   $2^+$  state.

Shell	Operator <sup>a</sup>	$Z_0^b$	$Z_1^b$	$A_0^c$	$A_1^c$
$p$	(11)	-0.1812	-0.1801	3.11	
$sd$	(11)	-0.7445	0.0017	19.05	-7.62
$sd$	(22)	-0.2321	0.0006		-0.64
				22.16	-8.26
$p$	(11)	0.4245	0.4229	7.29	
$sd$	(11)	-0.0007	0.0048	-0.04	0.02
$sd$	(22)	-0.0492	0.0046		-0.13
				7.25	-0.11

<sup>a</sup> $\text{SU}_3$  quantum numbers of  $a^\dagger a$  coupled to  $(\lambda\mu)$   $\Delta L=2$ ,  $\Delta S=0$ ; for (11), in the  $sd$  shell, the polynomial is  $1 - \frac{2}{3}y$ ; for (22) in the  $sd$  shell, the combination of  $K=0$  and  $K=2$  that gives a nonvanishing form factor is listed; small contributions involving  $pf$  orbits are omitted.

<sup>b</sup>One-body density-matrix elements reduced in  $J$  but not  $T$ .

<sup>c</sup>Polynomial coefficients of Eq. (2) for  $b = 1.821$  fm and effective charges,  $\delta e_p = \delta e_n = 0.5$ .

( $d_{5/2}d_{3/2}$ ) and 10.0 MeV ( $s_{1/2}d_{3/2}$ ). We expect the spacings of states within bands to be roughly maintained in shell-model calculations that use an expanded basis or slightly different interaction; interestingly, the strongly excited normal-parity state at 11.65 MeV shown in Fig. 2, is near the  $K=2$   $4^+$  state predicted to lie at 11.50 MeV. Preliminary measurements<sup>29</sup> of its form factor are consistent in shape with a  $4^+$  assignment; however, the strong excitation of this state is not presently understood and all we can say with confidence is that  $J \leq 4$ .

The shell-model basis, for the calculation already described, was chosen to give a good account of the coupling of two  $p$ -shell holes to the  $T=0$  states of the  $^{20}\text{Ne}$  ground-state band with mainly [4] symmetry for the four  $sd$ -shell nucleons. A pair of  $p$ -shell holes, with either spatial symmetry, can couple to four nucleons with [31] symmetry, of which the lowest  $T=1$  states are examples, to form  $4p2h$  states that also have [ $4^4_2$ ] symmetry and therefore  $S=0$  for  $T=1$ . From the same couplings,  $4p2h$  states with [ $4^4_{11}$ ] or [ $4^3_{33}$ ] symmetry and  $S=1$  for  $T=1$  can be formed. For each coupling of symmetries, specific weightings of the various  $T_p S_p \otimes T_h S_h$  possibilities are implied, including combinations with  $T_p=0$  or  $T_h=0$ ; thus, since the effective interaction favors high spatial symmetries, the lowest state with mainly [31] symmetry for ( $sd$ )<sup>4</sup> may have a somewhat different structure from that used for our simple weak-coupling estimates in the Introduction. Indeed, we find that the first band structure apart from the “(82)” bands is a  $K=1$  band with  $S=0$ , mainly from the (63) representation with appreciable (71) components. The  $1^+$  and  $2^+$  members are around 11.3 MeV, about 2–3 MeV higher than the candidate states discussed in this paper. Calculations with a basis large enough to incorporate the  $sd$ -shell and cross-shell correlations important for the energies of such states are necessary as the next step towards an understanding of states above 8-MeV excitation energy in  $^{18}\text{O}$ .

Finally, with regard to the 9.36-MeV  $2^+$  level, it is of interest to consider the theoretical prediction for the transverse form factor. The transverse form factor for the  $^{14}\text{C}$  core transition has been measured by Plum.<sup>30</sup> In fact, the mixed  $0p2h$  and  $2p4h$   $2^+$  states in  $^{14}\text{C}$  at 7.01 and 8.32 MeV, respectively, have very similar transverse form factors; the total transverse strength is understood if the magnetization current contribution to  $F_T$  is quenched by a factor of  $\sim 0.7$ , as was necessary<sup>28</sup> for  $E2$  transitions in  $^{13}\text{C}$ . There is little  $sd$ -shell contribution to  $F_T$  in  $^{14}\text{C}$ , but we note that such contributions play a role in the longitudinal form factor<sup>30,31</sup> with constructive (destructive) interference between  $p$ -shell and  $sd$ -shell contributions for the lower (upper)  $2^+$  state. The magnetization current contributions to the  $E2$  form factor are controlled by the  $\Delta L=2, \Delta S=1$  OBDME (one-body density-matrix element). For the  $4p2h$   $0^+ \rightarrow K=2$   $2^+$  transition in  $^{18}\text{O}$ , the  $p$ -shell OBDME dominates with  $Z_0=Z_1=-0.2075$ , to be compared with  $-0.3065$  for the simple  $0p2h$  transition in  $^{14}\text{C}$ . The polynomial coefficient  $B_1$  in Eq. (3) is easily evaluated using the results in Appendix A of Ref. 28. For a 15%  $4p2h$  admixture in the  $^{18}\text{O}$  ground state and a quenching factor of  $1/\sqrt{2}$ , we have  $B_1=4.52 \text{ efm}^2$ , with  $B_0=1.5 \text{ efm}^2$  from the continuity equation. The

TABLE VII. Expansion coefficients (in  $\text{efm}^4$ ) for the longitudinal and transverse electric form factors of the  $4^+$  states in  $^{18}\text{O}$  at 3.55 and 7.12 MeV (fitted to 48 and 38 data points, respectively). The value of the oscillator parameter  $b$  is 1.879 fm (see Table III).

Quantity	$4_1^+$	$4_1^+$	$4_1^+$	$4_2^+$
$A_0$	31.13(56)	31.28(55)	31.34(61)	113.8(15)
$A_1$	-1.38(24)	-1.41(21)	-1.29(22)	-13.1(6)
$B_1$	94(15)	-122(15)	0	-55(81)
$\chi^2/\nu$	1.20	1.17	1.45	2.26

core polarization corrections that quench the peak values of magnetization-current dominated  $E2$  form factors are also expected to make the form factors hold up above the simple  $p$ -shell form factor at high  $q$ .<sup>28,32</sup>

### C. $4^+$ levels

The form factors of the first two  $4^+$  states in  $^{18}\text{O}$ , at 3.55 and 7.12 MeV, were measured and analyzed by Norum *et al.*,<sup>2</sup> within the framework of the model of Lawson, Serduke, and Fortune (LSF).<sup>7</sup> Subsequently, a state in  $^{18}\text{O}$  at 9.0 MeV has been identified as the predominantly  $d_{5/2}d_{3/2}$   $4^+$  state.<sup>10</sup> This state is not observed in our experiment and we try to understand this fact, and the form factors of the levels at 3.55 and 7.12 MeV, within the framework of shell-model calculations.

The expansion coefficients obtained from fitting the data for the  $4_1^+$  and  $4_2^+$  levels are given in Table VII. Figure 5 shows the extracted Coulomb form factors for these levels with curves corresponding to the fitted coefficients in columns 1 and 4 of Table VII. For both levels,  $A_0$  is well determined. The inclusion of  $B_1$  in the fit leads to an improved  $\chi^2$  for the  $4_1^+$  level. Because  $|B_{1y}| > |B_0|$  over

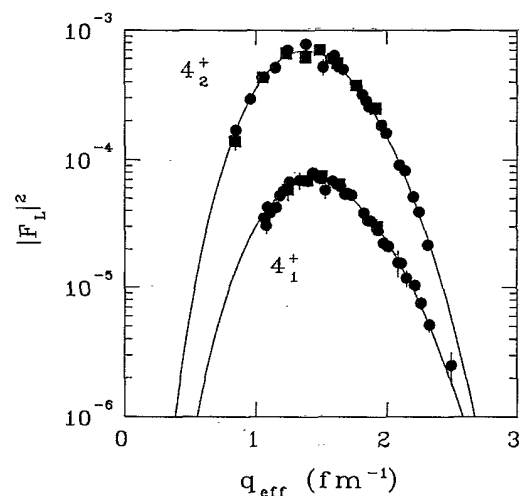


FIG. 5. The solid curves show the fitted Coulomb form factors for the  $4^+$  states in  $^{18}\text{O}$  at 3.56 MeV ( $4_1^+$ ) and 7.12 MeV ( $4_2^+$ ). Solid squares indicate measurements from this analysis and solid circles indicate measurements from an earlier analysis.<sup>2</sup>

TABLE VIII. One-body density-matrix elements ( $1d \rightarrow 1d$ ) for pure  $2p0h$  and  $4p2h$   $0^+ \rightarrow 4^+$  transitions in  $^{18}\text{O}$ .  $\text{CW}_n$  denotes a state from Table I;  $2\hbar\omega$  denotes the lowest  $2\hbar\omega$  state.  $Z_0$  and  $Z_1$  are defined in Table VI.

$4^+$	$\leftarrow$	$0^+$	$\Delta L=4, \Delta S=0$		$\Delta L=4, \Delta S=1$	
			$Z_0$	$Z_1$	$Z_0$	$Z_1$
$\text{CW}_1$		$\text{CW}_1$	0.3063	-0.3063	-0.0445	0.0445
$\text{CW}_2$		$\text{CW}_1$	0.2325	-0.2325	-0.1385	0.1385
$(d_{5/2})^2$		$\text{CW}_1$	0.2235	-0.2235	0	0
$d_{5/2}d_{3/2}$		$\text{CW}_1$	0.3173	-0.3173	-0.1450	0.1450
$2\hbar\omega$		$2\hbar\omega$	0.4650	0.0002	-0.0200	0.0005

the range of  $q$  for which data exist, there are comparable fits for either sign of  $B_1$ . The fit for  $(B_1 B_0) < 0$ , as expected theoretically (and discussed in the following), has a slightly better  $\chi^2$ . For the  $4_2^+$  level,  $B_1$  is undetermined.

The OBDME relevant to the computation of  $C4$  and  $E4$  form factors for the two  $(sd)^2$  states and the lowest  $4p2h$  state are given in Table VIII. For the  $(sd)^2$  states, let  $\alpha, \beta$  denote the  $(d_{5/2})^2, (d_{3/2})^2$  amplitudes in a  $0^+$  state and  $\alpha', \beta'$  denote the  $(d_{5/2})^2, d_{5/2}d_{3/2}$  amplitudes in a  $4^+$  state. Then,

$$Z_0(\Delta L=4, \Delta S=0) = \frac{1}{\sqrt{15}}\alpha\alpha' + \frac{1}{\sqrt{10}}\beta\beta' + \frac{1}{\sqrt{15}}\alpha\beta', \quad (6)$$

$$Z_1(\Delta L=4, \Delta S=1) = -\frac{1}{\sqrt{12}}\alpha\beta' + \frac{1}{\sqrt{8}}\beta\beta', \quad (7)$$

which makes explicit the sensitivity to the  $(d_{3/2})^2$  component in the ground state and to the mixing of  $(d_{5/2})^2$  and  $d_{5/2}d_{3/2}$  in the excited states. Values of  $A_0$  and  $B_1$  for each of the cases in Table VIII can be evaluated from

$$A_0 = 15.93 b^4 (e_0 Z_0 + e_1 Z_1), \quad (8)$$

$$B_1 = -5.9935 \frac{\hbar c}{E_x} b^2 Q (\mu_0 Z_0 + \mu_1 Z_1), \quad (9)$$

where  $e_0 = 1 + \delta e_p + \delta e_n$ ,  $e_1 = 1 + \delta e_p - \delta e_n$ ,  $\mu_0 = \mu_p + \mu_n = 0.880$ ,  $\mu_1 = \mu_p - \mu_n = 4.706$ , and  $Q$  is a quenching factor for the  $\Delta S=1$  excitation. From an analysis of  $E4$  transition probabilities in the  $sd$  shell, Brown *et al.*<sup>33,34</sup> have found  $e_0 \approx 2$ , while the microscopic calculations of Sagawa and Brown<sup>35</sup> give  $\delta e_n = 0.6$ ,  $\delta e_p = 0.3$ . To make rough estimates for  $A_0$ , we use  $\delta e_p = \delta e_n = 0.5$  and

$b = 1.879$  fm. For  $B_1$ , we set  $Q = 1/\sqrt{2}$ , as we did for  $E2$  transitions, to represent the empirical quenching of spin excitations.

Table IX gives the wave functions of the three  $4^+$  states from the "unconstrained II" version of the LSF model<sup>7</sup> and from our shell-model calculation. The two sets of wave functions are very similar except for the increased mixing of the  $(d_{5/2})^2$  and  $d_{5/2}d_{3/2}$  configurations in the shell-model calculation, a consequence of using the CW interaction for the  $sd$  shell. We take the  $^{18}\text{O}$  ground-state wave function to be a mixture of the first CW  $0^+$  state (Table I) and the  $2\hbar\omega$   $0^+$  state. We do this because the LSF model omits  $(d_{3/2})^2$  components from the ground-state wave function (see footnote to Table IX) and because we believe that the  $2\hbar\omega$  intensity in the ground state is larger than that given by the LSF model. Evidence for the latter is supported by the fact that the  $B(C2)\uparrow$  for the  $2_3^+$  state determined from electron scattering is a factor of three larger than that given by the LSF model and that the accepted value<sup>1</sup> of  $B(C2)\uparrow$  for the  $2_1^+$  state is now about 25% larger than the value used in the LSF analysis.

From Eq. (8) and Table VIII, the  $A_0$  values for  $\text{CW}(0^+) \rightarrow (d_{5/2})^2(4^+)$ ,  $2\hbar\omega(0^+) \rightarrow 2\hbar\omega(4^+)$ , and  $\text{CW}(0^+) \rightarrow d_{5/2}d_{3/2}(4^+)$  are 44.4, 184.7, and 63.0  $\text{efm}^4$ , respectively. Taking a ground-state wave function of the form  $\sqrt{0.85} \text{CW}(0^+) + \sqrt{0.15} 2\hbar\omega$ , we find for the LSF  $4^+$  wave functions from Table IX:

$$A_0(4_1^+) = 40.4 + 4.6 + 8.8 = 53.8,$$

$$A_0(4_2^+) = 4.9 - 65.2 - 22.8 = -83.1,$$

$$A_0(4_3^+) = -4.6 - 28.9 + 52.7 = 19.2,$$

TABLE IX. Wave functions for the first three  $4^+$  states in  $^{18}\text{O}$  for the model of Lawson, Serduke, and Fortune (LSF) and our shell-model calculation.

Model	LSF <sup>a</sup>			Shell Model <sup>b</sup>			
	$J_n^\pi$	$(d_{5/2})^2$	$2\hbar\omega$	$d_{5/2}d_{3/2}$	$(d_{5/2})^2$	$2\hbar\omega^c$	$d_{5/2}d_{3/2}$
$4_1^+$		0.986	0.065	0.151	0.918	0.098	0.335
$4_2^+$		0.120	-0.912	-0.392	0.242	-0.888	-0.373
$4_3^+$		-0.113	-0.404	0.908	-0.285	-0.445	0.805

<sup>a</sup>Constrained II wave functions from Ref. 7 with the phase of the  $2\hbar\omega$  component adapted to our convention. The ground-state wave function for the same fit is  $0.848 (d_{5/2})^2 + 0.438 (s_{1/2})^2 + 0.297 2\hbar\omega$ .

<sup>b</sup>Wave functions are not normalized because the amplitudes listed represent only three components of a much larger basis. The ground state has 4.1%  $2\hbar\omega$  components and 95.9%  $\text{CW}_1$  of Table I.

<sup>c</sup>The  $2\hbar\omega$  amplitudes listed represent only the contributions from the lowest " $K=0$ "  $2\hbar\omega$  state.



where the individual contributions from each basis state are given in the order of Table IX. An important point to note is the strong cancellation for the  $4_3^+$  level (almost complete for the shell-model  $4^+$  wave functions); also,  $A_0(4_1^+)$  is too large and  $A_0(4_2^+)$  is too small compared to the values deduced from the  $(e, e')$  form factors (Table VII). The most obvious way to improve the agreement with experiment would be for the matrix element that mixes the lowest  $(sd)^2 4^+$  state and the  $2\hbar\omega$  state to change sign. This matrix element is small and it is clear that a small admixture of the opposite sign would be sufficient to give rather good agreement with experiment. Whether such a sign change could reasonably be obtained requires a much more detailed analysis and extended shell-model calculations. It is of interest to note that of the 4.1%  $2\hbar\omega$  admixture in the lowest  $4^+$  model state, less than 1% is from the lowest " $K=0$ "  $2\hbar\omega$  state; most of the  $2\hbar\omega$  admixture involves configurations in which the four  $sd$ -shell nucleons are coupled to  $T=1$ .

The  $2\hbar\omega$  admixtures make little contribution to the transverse form factors of the  $4^+$  levels (see Table VIII). The dominant magnetization current contributions to the transverse form factors are then a measure of the  $d_{5/2}d_{3/2}$  component for each level. For the lowest  $4_1^+$  level, the shell-model wave functions give  $B_1 \approx -142 \text{ efm}^4$ , which is consistent with the fitted value in Table VII, while the LSF value is about a factor of two smaller. The peak value of  $|F_T|^2$  obtained from the fit is  $7.8 \times 10^{-7}$  at  $q_{\text{eff}} = 1.7 \text{ fm}^{-1}$ , two orders of magnitude smaller than the peak value of  $|F_L|^2$ . For the third  $4^+$  level, the peak value of  $|F_T|^2$  should be about  $8 \times 10^{-6}$ . This form factor should be measurable at  $180^\circ$  if the  $4_3^+$  state were an isolated level; however, it may not be measurable for a relatively broad level at 9.0 MeV in  $^{18}\text{O}$ .

### III. SUMMARY AND CONCLUSIONS

We have presented the first high-resolution form-factor measurements for the  $2^+$  state at 8.21 MeV and for a normal-parity state at 9.36 MeV, which we suggest is also

a  $2^+$  state. The measurements are construed as evidence that these levels are basically  $4p2h$  states; properties of  $2p0h$  states are inconsistent with the data. Weak-coupling arguments suggest that the states are  $K=2$  bandheads for levels of the type  $p^{-2} \otimes (sd)^4$ , where the four  $sd$ -shell nucleons couple to  $T=1$  and  $T=0$  for the 8.21- and 9.36-MeV levels, respectively. In terms of  $\text{SU}_3$  symmetry, the dominant representations in these bands are (63) and (82). We have noted the effective interaction will tend to mix the simple weak-coupling configurations in such a way that the lowest states have high spatial symmetry, in which case the lowest (63) configurations should have  $S=0$  and  $K=1$ . Although we have attempted to match the observed states with theoretical candidates on the basis of excitation energies and the shapes and magnitudes of form factors, our assignments are not definitive. Larger basis shell-model calculations are necessary to investigate whether the weak-coupling or the symmetry-preserving characteristics of the interaction prevail.

The results of existing calculations were compared to data for the first three  $4^+$  states at 3.55, 7.12, and 9.0 MeV. While the shapes and relative magnitudes of these states are qualitatively understood within the framework of these calculations, it will be interesting to see if extended-basis calculations can account for the known  $4^+$  state at 10.3 MeV and whether the presence of this state or other low-lying  $4^+$  levels influence the mixing and properties of the two lowest  $4^+$  levels.

### ACKNOWLEDGMENTS

The authors thank the technical staff at the MIT-Bates Linear Accelerator Center for their support during the experiment. This work was supported in part by the U.S. Department of Energy under Contract Nos. DE-AC02-76ER03069, DE-AC02-76CH00016, and DE-FG05-86ER40285 and by the National Science Foundation under Grant Nos. PHY-8501054 and PHY-8902479.

<sup>(a)</sup>Present address: IBM Corporation, General Technology Division, Hopewell Junction, NY 12533.

<sup>(b)</sup>Present address: Department of Physics, College of William and Mary, Williamsburg, VA 23185.

<sup>(c)</sup>Present address: Department of Physics, University of New Hampshire, Durham, NH 03824.

<sup>(d)</sup>Present address: Department of Physics, University of Washington, Seattle, WA 98195.

<sup>(e)</sup>Present address: Los Alamos National Laboratory, Los Alamos, NM 87545.

<sup>(f)</sup>Present address: Department of Physics and Astronomy, University of Maryland, College Park, MD 20742.

<sup>(g)</sup>Present address: Department of Physics, University of Kentucky, Lexington, KY 40506.

<sup>(h)</sup>Present address: Department of Physics, University of Virginia, Charlottesville, VA 22901.

<sup>(i)</sup>Present address: Tektronics Inc., Beaverton, OR 97077.

<sup>(j)</sup>Present address: Department of Physics, Luther College, Decorah, IA 52101.

<sup>(k)</sup>Retired.

<sup>1</sup>F. Ajzenberg-Selove, Nucl. Phys. **A475**, 1 (1987).

<sup>2</sup>B. E. Norum, M. V. Hynes, H. Miska, W. Bertozzi, J. Kelly, S. Kowalski, F. N. Rad, C. P. Sargent, T. Sasanuma, W. Turchinets, and B. L. Berman, Phys. Rev. C **25**, 1778 (1982).

<sup>3</sup>J. Kelly, W. Bertozzi, T. Buti, M. Deady, F. W. Hersman, C. Hyde, M. V. Hynes, S. Kowalski, J. Lichtenstadt, B. Norum, B. Pugh, F. N. Rad, R. Redwine, A. Bacher, G. Emery, C. Foster, W. Jones, D. Miller, B. L. Berman, F. Petrovich, and W. G. Love, Los Alamos Scientific Laboratory Report No. LA-8303-C, 1980.

<sup>4</sup>S. J. Seestrom-Morris, D. Dehnhard, M. A. Franey, D. B. Holtkamp, C. L. Blilie, C. L. Morris, J. D. Zumbro, and H. T. Fortune, Phys. Rev. C **37**, 2057 (1988).

<sup>5</sup>J. Kelly, W. Bertozzi, T. N. Buti, J. M. Finn, F. W. Hersman, M. V. Hynes, C. Hyde-Wright, B. E. Norum, A. D. Bacher, G. T. Emery, C. C. Foster, N. P. Jones, D. W. Miller, B. L. Berman, J. A. Carr, and F. Petrovich, Phys. Lett. **169B**, 157 (1986); and (unpublished).

- <sup>6</sup>A. C. Hayes, P. J. Ellis, and D. J. Millener (unpublished).
- <sup>7</sup>R. L. Lawson, F. J. D. Serduke, and H. T. Fortune, *Phys. Rev. C* **14**, 1245 (1976).
- <sup>8</sup>D. M. Manley, B. L. Berman, W. Bertozzi, T. N. Buti, J. M. Finn, F. W. Hersman, C. E. Hyde-Wright, M. V. Hynes, J. J. Kelly, M. A. Kovash, S. Kowalski, R. W. Lourie, B. Murdock, B. E. Norum, B. Pugh, C. P. Sargent, and D. J. Millener (unpublished).
- <sup>9</sup>W. Chung, Ph.D. thesis, Michigan State University, 1976.
- <sup>10</sup>H. T. Fortune, L. C. Bland, and W. D. M. Rae, *J. Phys. G* **11**, 1175 (1985); M. E. Coburn, L. C. Bland, H. T. Fortune, G. E. Moore, S. Mordechai, and R. Middleton, *Phys. Rev. C* **23**, 2387 (1981).
- <sup>11</sup>W. D. M. Rae, N. S. Godwin, D. Sinclair, H. S. Bradlow, P. S. Fisher, J. D. King, A. A. Pilt, and G. Proudfoot, *Nucl. Phys. A* **319**, 239 (1979).
- <sup>12</sup>T. N. Buti, J. Kelly, W. Bertozzi, J. M. Finn, F. W. Hersman, C. Hyde-Wright, M. V. Hynes, M. A. Kovash, S. Kowalski, R. W. Lourie, B. Murdock, B. E. Norum, B. Pugh, C. P. Sargent, W. Turchinets, and B. L. Berman, *Phys. Rev. C* **33**, 755 (1986).
- <sup>13</sup>R. Bansal and J. B. French, *Phys. Lett.* **11**, 145 (1964); L. Zamick, *ibid.* **19**, 580 (1965).
- <sup>14</sup>D. M. Manley, B. L. Berman, W. Bertozzi, T. N. Buti, J. M. Finn, F. W. Hersman, C. E. Hyde-Wright, M. V. Hynes, J. J. Kelly, M. A. Kovash, S. Kowalski, R. W. Lourie, B. Murdock, B. E. Norum, B. Pugh, and C. P. Sargent, *Phys. Rev. C* **36**, 1700 (1987).
- <sup>15</sup>A. H. Wapstra and K. Bos, *At. Data Nucl. Data Tables* **19**, 177 (1977).
- <sup>16</sup>W. L. Bendel, L. W. Fagg, S. K. Numrich, E. C. Jones, Jr., and H. F. Kaiser, *Phys. Rev. C* **3**, 1821 (1971).
- <sup>17</sup>C. Djalali, G. M. Crawley, B. A. Brown, V. Rotberg, G. Caskey, A. Galonsky, N. Marty, M. Morlet, and A. Willis, *Phys. Rev. C* **35**, 1201 (1987).
- <sup>18</sup>D. Bender, A. Richter, E. Spamer, E. J. Ansaldo, C. Rangacharyulu, and W. Knüpfer, *Nucl. Phys. A* **406**, 504 (1983).
- <sup>19</sup>B. A. Brown, W. Chung, and B. H. Wildenthal, *Phys. Rev. C* **22**, 774 (1980).
- <sup>20</sup>H. Miska, B. Norum, M. V. Hynes, W. Bertozzi, S. Kowalski, F. N. Rad, C. P. Sargent, T. Sasanuma, and B. L. Berman, *Phys. Lett.* **83B**, 165 (1979).
- <sup>21</sup>M. Gai, R. Keddy, D. A. Bromley, J. W. Olness, and E. K. Warburton, *Phys. Rev. C* **36**, 1256 (1987).
- <sup>22</sup>J. A. Weinman and E. A. Silverstein, *Phys. Rev.* **111**, 277 (1958).
- <sup>23</sup>J. J. Kelly, W. Bertozzi, F. W. Hersman, M. V. Hynes, B. E. Norum, A. D. Bacher, G. T. Emery, C. C. Foster, W. P. Jones, D. W. Miller, B. L. Berman, and D. J. Millener (unpublished).
- <sup>24</sup>J. J. Kelly, W. Bertozzi, T. N. Buti, J. M. Finn, F. W. Hersman, C. Hyde-Wright, M. V. Hynes, M. A. Kovash, B. Murdock, B. E. Norum, B. Pugh, F. N. Rad, A. D. Bacher, G. T. Emery, C. C. Foster, W. P. Jones, D. W. Miller, B. L. Berman, W. G. Love, J. A. Carr, and F. Petrovich, *Phys. Rev. C* **39**, 1222 (1989); K. Amos, W. Bauhoff, I. Morrison, S. F. Collins, R. S. Henderson, B. M. Spicer, G. G. Shute, V. C. Officer, D. W. Devins, D. L. Friesel, and W. P. Jones, *Nucl. Phys. A* **413**, 255 (1984).
- <sup>25</sup>G. L. Morgan, D. R. Tilley, G. E. Mitchell, R. A. Hilko, and N. R. Roberson, *Phys. Lett.* **32B**, 353 (1970).
- <sup>26</sup>A. Cunsolo, A. Foti, G. Immè, G. Pappalardo, G. Raciti, and N. Saunier, *Phys. Rev. C* **24**, 476 (1981); *Phys. Lett.* **112B**, 121 (1982); *Lett. Nuovo Cimento* **37**, 193 (1983).
- <sup>27</sup>L. Kraus, I. Linck, and J. C. Sens (unpublished).
- <sup>28</sup>D. J. Millener, D. I. Sober, H. Crannell, J. T. O'Brien, L. W. Fagg, S. Kowalski, C. F. Williamson, and L. Lapikás, *Phys. Rev. C* **39**, 14 (1989).
- <sup>29</sup>R. M. Sellers, D. M. Manley, R. A. Lindgren, M. Farkhondeh, B. E. Norum, B. L. Clausen, R. J. Peterson, C. E. Hyde-Wright, B. L. Berman, and D. J. Millener (unpublished).
- <sup>30</sup>M. A. Plum, Ph.D. dissertation, University of Massachusetts, 1985; M. A. Plum, R. A. Lindgren, J. Dubach, R. S. Hicks, R. L. Huffman, B. Parker, G. A. Peterson, J. Alster, J. Lichtenstadt, M. A. Moinester, and H. Baer, *Phys. Rev. C* **40**, 1861 (1989).
- <sup>31</sup>H. Crannell, P. L. Hallowell, J. T. O'Brien, J. M. Finn, F. J. Kline, S. Penner, J. W. Lightbody, Jr., and S. P. Fivozinsky, supplement to Research Report of Laboratory for Nuclear Science, Tohoku University, 1972.
- <sup>32</sup>T. Sato, K. Koshigiri, and H. Ohtsuko, *Z. Phys. A* **320**, 507 (1985).
- <sup>33</sup>B. A. Brown, W. Chung, and B. H. Wildenthal, *Phys. Rev. C* **21**, 2600 (1980).
- <sup>34</sup>B. A. Brown, R. Rahdi, and B. H. Wildenthal, *Phys. Rep.* **101**, 313 (1983).
- <sup>35</sup>H. Sagawa and B. A. Brown, *Phys. Lett.* **150B**, 247 (1985).